PERGAMON

Electrochimica Acta 44 (1998) 643–651

ELECTROCHIMICA Acta

The influence of UV light on the dissolution and passive behavior of copper-containing alloys in chloride solutions

Carmel B. Breslin, Digby D. Macdonald *, [1]

Center for Advanced Materials, The Pennsylvania State University, 517 Deike Building, University Park, PA 16802, U.S.A.

Received 2 February 1998

Abstract

The influence of UV light (300–450 nm) on the passive and dissolution behavior of copper alloys CA-715 and CDA-614 in dilute chloride-containing solutions was studied. A slight ennoblement in the breakdown potential, an increase in the induction time, and considerably reduced anodic current densities at potentials higher that the initial breakdown potential were observed for the illuminated electrode. These effects were observed regardless of whether the electrodes were illuminated continuously or illuminated only before the polarization scans, and appear to be independent of the wavelength of the incident light in the wavelength region 300 to 450 nm. These findings are explained in terms of a photo-induced modification of the passive film formed on the copper-containing alloys in the dilute chloride solution, which render it more resistant to the onset of attack. This modification is explained in terms of the semiconducting nature of the passive film and the point defect model for the breakdown of passivity.

Keywords: Copper alloys; Pitting corrosion; Pitting; Photoinhibition; Dissolution

1. Introduction

Copper-based alloys exhibit an attractive combination of properties, such as a high resistance to corrosion and good thermal and electrical conductivities, and thus it is not surprising that these alloys find widespread application in many environments. The oxide layers formed on copper and many copper-based alloys have been described in terms of a duplex structure, an inner Cu_2O and an outer hydrated layer, ranging in composition from CuO to $Cu(OH)_2$ [1–7]. In neutral, or acidic, chloride-containing solutions, copper alloys electro-oxidize to form cuprous chloride complexes [8, 9].

Nickel is frequently added as an alloying addition to copper in order to increase the resistance of the alloy towards localized corrosion [10]. The corrosion and electrochemical behavior of these nickel based copper alloys is characterized by the individual properties of both alloying components. The passive layer formed on copper–nickel alloys depends on the solution composition, applied potential, and pH, but generally consists of an inner oxide and an outer hydroxide component, with hydroxide species, such as $Ni(OH)_2$, NiO, NiOOH, CuO and Cu_2O and $Cu(OH)_2$ being identified in the hydroxide layer [11].

Crystalline Cu_2O is a p-type semiconductor with a band-gap energy of 2.2 to 2.3 eV [12]. Several reports in the literature have shown that copper oxide passive films exhibit p-type semiconductivity [13–15] and that under illumination conditions the copper

* Author to whom correspondence should be addressed. Tel. +1 650 326 3195; Fax: +1 650 859 3250; e-mail: digby@unix.sri.com

[1] Permanent address: Dept. Chemistry, National University of Ireland, Maynooth, Co. Kildare, Ireland.

0013-4686/98/$19.00
PII: S0013-4686(98)00109-1

oxide is photo-reduced [13, 16]. However, there is evidence to suggest that in chloride-containing solutions a CuCl film is formed which exhibits n-type semiconductivity [17], while in other cases photo-responses characteristic of simultaneous p-type and n-type behavior have been reported [13, 18–20], illustrating the complex nature of these oxide layers.

It has been shown that copper can exhibit stress-corrosion cracking in the dark, but not under illumination conditions [21]. In the case of pure nickel, it has been shown that illumination leads to an increased resistance to the onset of pitting corrosion [22]. Indeed, a similar photo-induced inhibition of pitting attack has been reported for pure iron [23] and iron-based alloys [24–26].

In this paper, the results of a study on the influence of UV light on the dissolution and passive behavior of two copper-based alloys, CA-715 (70Cu30Ni) and CDA-614 (91Cu7Al2Fe), in a dilute buffered chloride solution, are reported. These materials, a copper–nickel alloy and a copper alloy but without any nickel addition, were selected for study because of the photo-induced effects reported previously for pure copper and nickel.

2. Experimental

Test specimens were prepared from CA-715 (70Cu30Ni) CDA-614 (91Cu7Al2Fe), and pure copper (99.98%) rods, which were covered with lacquer, mounted in a PVC holder and embedded in a two-component epoxy resin. The exposed surfaces, approximately 0.8 cm^2 in area (0.796 cm^2 for all Cu electrodes and 0.83 cm^2 for all CA-715 and CDA-614 electrodes), were polished mechanically with successively finer grades of SiC paper and finally to a mirror finish with 0.05 μ alumina powder. The surfaces were then cleaned ultrasonically with distilled water.

A three-electrode PTFE cell equipped with a quartz window, to allow irradiation of the test electrodes, was used as the test cell. A saturated calomel electrode was used as the reference electrode and a platinum wire, coiled inside the PTFE cell, was used as the auxiliary electrode. Test solutions, 0.025 mol dm^{-3} NaCl, were prepared from AnalaR-grade reagents and de-ionized water. The pH of the solutions was adjusted to 7.8 with a 0.15 mol dm^{-3} H_3BO_3/0.007 mol dm^{-3} $Na_2B_4O_7$ buffer solution.

The working electrodes were irradiated at wavelengths between 300 and 450 nm using a 150 W UV-enhanced Xe lamp (Oriel model 6254) and a 1/8 monochromator (Oriel model 77250). The incident power density at 300 nm was 400 mW cm^{-2}, giving a photon flux of 6.0×10^{14} cm^{-2}. The photon flux was maintained at approximately this value at each wavelength by adjusting the light intensity at the surface using neutral density filters.

Electrochemical tests were carried out using a Solartron/Schlumberger ECI model 1286 potentiostat. In potentiodynamic polarization tests the working electrodes were polarized at a rate of 0.1 mV s^{-1} from −200 mV(SCE) in the anodic direction. The electrodes were immersed in solution immediately following the polishing regime and polarized at −200 mV(SCE) for 30 s. The electrodes were then polarized from −200 mV at the scan rate of 0.1 mV s^{-1} for the non-illuminated experiments, and polarized from −200 mV(SCE) at the scan rate of 0.1 mV s^{-1} under continuous illumination for the illumination experiments. The breakdown potential was recorded when the current exceeded 10 μA cm^{-2}. In current–time measurements, the electrodes were initially polarized at various applied potentials under conditions of illumination and non-illumination in a 0.15 mol dm^{-3} H_3BO_3/0.007 mol dm^{-3}

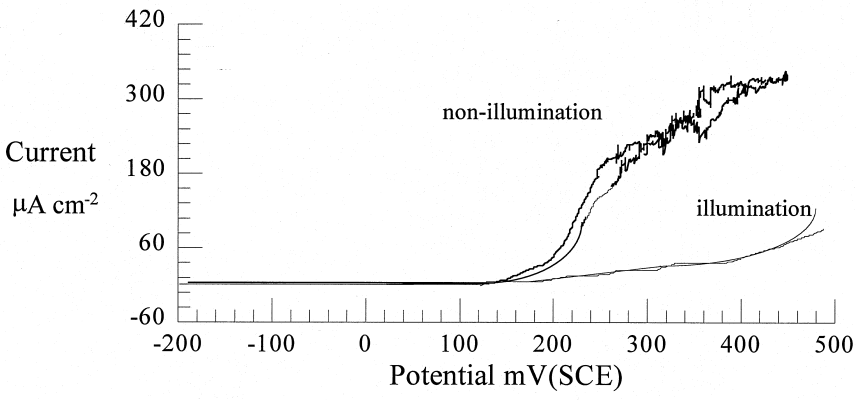

Fig. 1. Potentiodynamic polarization plots recorded for CA-715 in a buffered 0.025 mol dm^{-3} NaCl solution under conditions of continuous illumination at 300 nm and non-illumination.

$Na_2B_4O_7$ buffer solution; the specimens were then transferred to the buffered 0.025 mol dm^{-3} NaCl solution and the current–time transients were recorded in the dark at a sampling rate of 90 mS using a Keithley model 576 data acquisition unit.

3. Results

The potential–current plots, recorded at a scan rate of 0.1 mV s^{-1} and from a potential of −200 mV(SCE) for CA-715 under conditions of continuous illumination at 300 nm and non-illumination, are shown in Fig. 1. A total of four plots are shown (two representative plots for the non-illumination conditions and two for the illumination conditions) to illustrate the degree of reproducibility from experiment to experiment. It is evident from these profiles that illumination leads to a considerable reduction in the anodic current at applied potentials exceeding +200 mV(SCE). In addition, the current noise, probably associated with metastable breakdown events or the propagation of attack/precipitation of corrosion products, observed for the non-illuminated electrode is reduced considerably on illumination. The breakdown potential depended slightly on illumination. An anodic displacement in the breakdown potential of 30 ± 25 mV was observed on continuous illumination. This displacement was evaluated from a total of 20 experiments, 10 carried out in the dark and 10 performed under continuous illumination conditions.

In order to correlate this current–potential behavior with the nature of the surface attack, a number of experiments were carried out in which the alloys were polarized up to a predetermined potential, then removed from the solution, and the surface viewed under a high resolution optical microscope. These experiments were carried out for both illuminated and non-illuminated specimens. Localized attack was observed following the initial current increase. On continued polarization, a greater number of initiation sites could be seen and eventually attack spread over the surface to give the final appearance of shallow general-like dissolution. But, the rate at which this attack spread to consume the surface was reduced on illumination, consistent with the much lower currents observed on polarization of the specimens in the anodic direction.

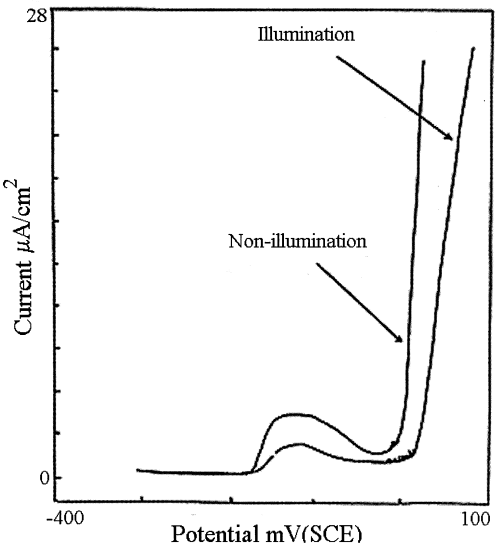

Fig. 2. Potentiodynamic polarization plots recorded for CDA-614 in a buffered 0.025 mol dm^{-3} NaCl solution under conditions of continuous illumination at 300 nm and non-illumination.

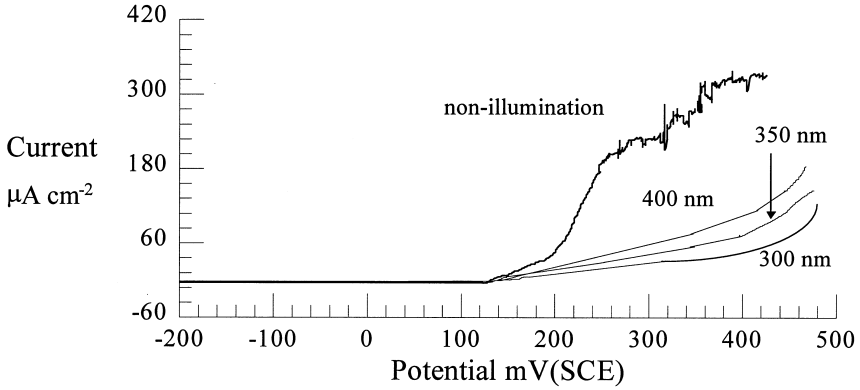

Fig. 3. Potentiodynamic polarization plots recorded for CA-715 in a buffered 0.025 mol dm^{-3} NaCl solution under conditions of continuous illumination at 300, 350 and 400 nm.

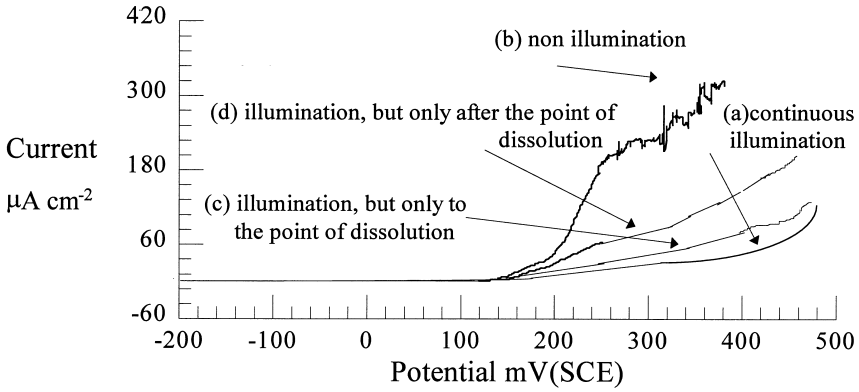

Fig. 4. Potentiodynamic polarization plots recorded for CA-715 in a buffered 0.025 mol dm^{-3} NaCl solution under conditions of (a) continuous illumination, (b) non-illumination, (c) illumination, but only up to the point where dissolution is first observed and (d) illumination from the point where dissolution is first observed.

Similar results were obtained with CDA-614. The current–potential behavior of this alloy in a buffered 0.025 mol dm^{-3} NaCl solution, under conditions of continuous illumination at 300 nm and non-illumination, are shown in Fig. 2. Again, it is seen that the anodic dissolution of the specimens at potentials above the breakdown potential is inhibited when illuminated. Likewise, the initial breakdown potential depended slightly on illumination being displaced by 25 ± 20 mV in the anodic direction on illumination.

The polarization behavior, in both cases, was found to vary only slightly with photon energy. In Fig. 3, the polarization plots, recorded for CA-715 in buffered 0.025 mol dm^{-3} NaCl solution, are shown as a function of wavelength. Here, it is seen that increasing the wavelength to 400 nm, decreases only marginally the resistance to anodic dissolution afforded by illumination.

It was found, also, for these systems, that continued illumination was not required to achieve resistance to dissolution. Polarization plots obtained for CA-715 under conditions of (a) continuous illumination, (b) non-illumination, (c) illumination, but only up to the point where dissolution is first observed, i.e. illumination from −200 mV to +190 mV, (d) illumination, but only after the point where dissolution is first observed, i.e. illumination from +190 mV to +500 mV, are shown in Fig. 4. These profiles indicate varying degrees of inhibition of dissolution. However, it is evident that illumination during the non-active period leads to some modification of the surface that influences the subsequent dissolution phase, and that dissolution can be somewhat inhibited in the active phase on illumination.

Further experiments involved the recording of current–time transients for CA-715 in a buffered 0.025 mol dm^{-3} NaCl solution following passivation under various conditions of illumination and non-illumination in the borate buffer solution. CA-715 alloys were polarized in the neutral borate buffer solution for periods up to 2 h at various applied potentials ranging from −100 to +600 mV(SCE) under conditions of illumination and non-illumination. There seemed to be no difference in the current–time plots recorded under conditions of illumination and non-illumination in this borate buffer solution. Following this film-formation period, the electrodes were transferred to a neutral buffered 0.025 mol dm^{-3} NaCl solution and the current–time transients were monitored at a constant potential of +100 mV(SCE) under non-illumination conditions. Typical current–time transients recorded at +100 mV(SCE) (in the dark) in the 0.025 mol dm^{-3} solution following film formation at +600 mV(SCE) for 2 h in the borate buffer solution under conditions of non-illumination and illumination are shown in Fig. 5(a) and (b), respectively, while the current–time data obtained following film formation at +200 mV(SCE) for 2 h under conditions of non-illumination and illumination are presented in Fig. 5(c) and (d), respectively. It is evident from a comparison of these figures that illumination during the film-formation period leads to more passive behavior. Also, it is seen that the specimens polarized at +600 mV(SCE) exhibit more passive behavior when compared to those polarized at +200 mV(SCE). The gradual current increases evident in Fig. 5(a) and (c) may be attributed to activation of the surface. The induction period, prior to the onset of activation, may be obtained by drawing a tangent to this increasing current, and intersecting it with the horizontal line marked by the current during the passive period. Using this approach, average induction periods

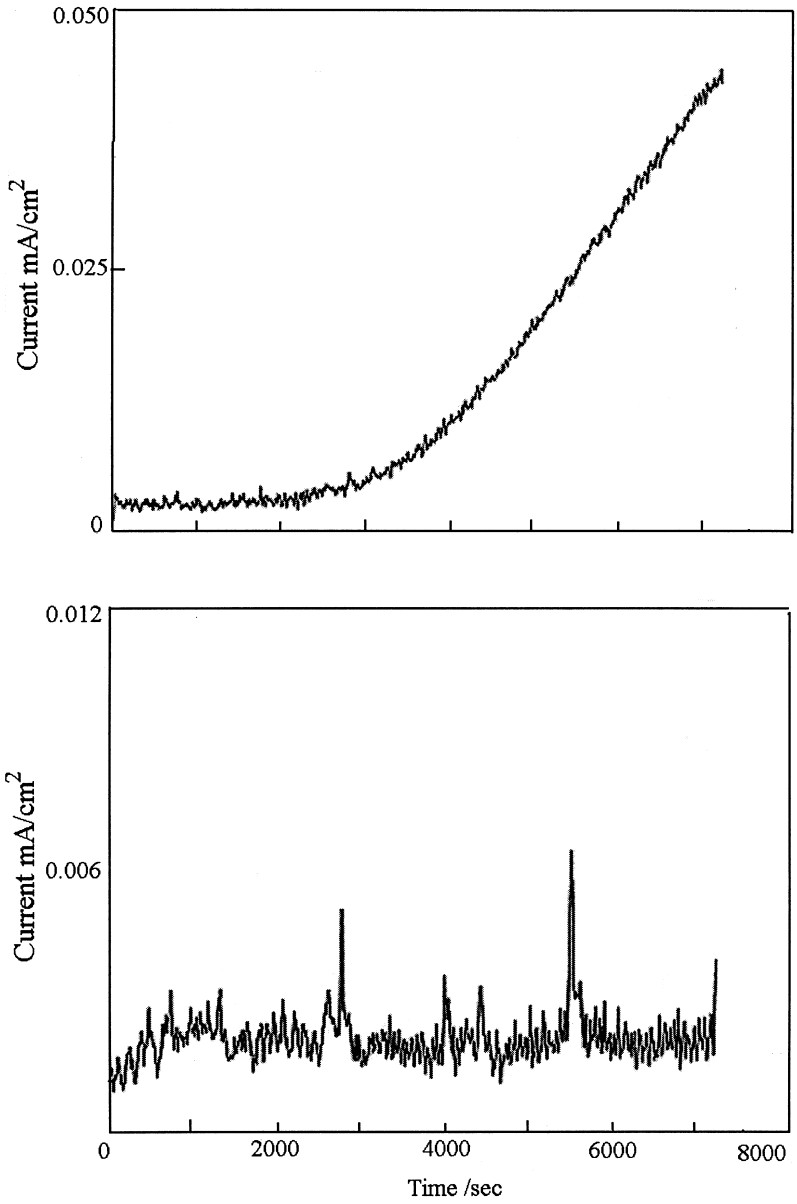

Fig. 5. *Caption overleaf.*

were calculated as 3000 ± 800 s and 9300 ± 1800 s for specimens pre-polarized at 200 mV(SCE) in the dark and in the light respectively, while the average induction periods calculated for the specimens pre-polarized at +600 mV(SCE) in the dark and in the light were 7000 ± 900 s and 17900 ± 3300 s respectively. These results, combined with the break down potential measurements, show that illumination during film formation leads to some modification of the passive film that subsequently leads to more passive behavior.

The breakdown potentials measured for pure copper under conditions of illumination and non-illumination in the buffered 0.025 mol dm^{-3} NaCl solution showed a poor degree of reproducibility. This may be connected to the fact that breakdown depended on a single initiation site and once this site was activated, surface attack seemed to emanate rapidly from this single location site; the rapid nature of attack being consistent with the favorable complexation reactions of copper and chloride. It was not possible to determine if illumination of the

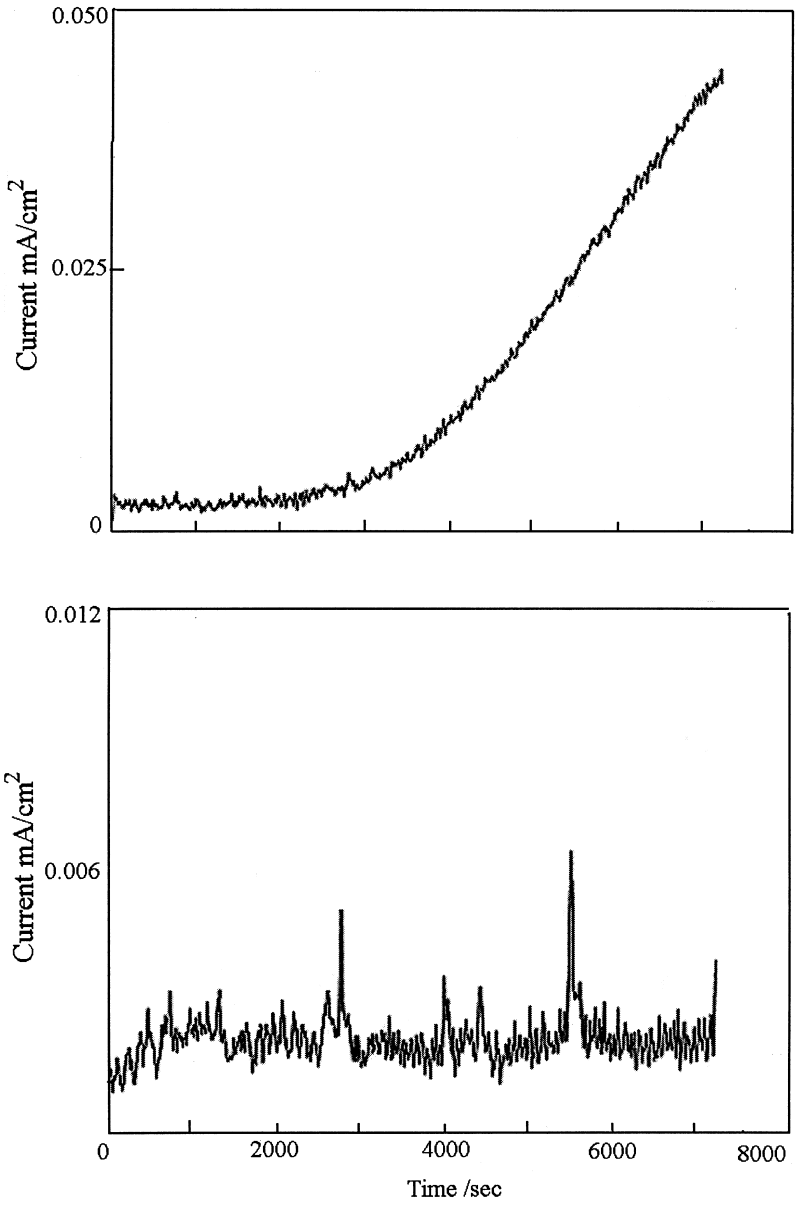

Fig. 5. Current–time transients recorded for CA-715 in a buffered 0.025 mol dm^{-3} NaCl solution at +100 mV(SCE) following (a) passivation at +600 mV(SCE) in a borate buffer solution for 120 min under non-illumination conditions, (b) passivation at +600 mV(SCE) in a borate buffer solution for 120 min under illumination conditions, (c) passivation at +200 mV(SCE) in a borate buffer solution for 120 min under non-illumination conditions and (d) passivation at +200 mV(SCE) in a borate buffer solution for 120 min under illumination conditions.

surface had any effect on the breakdown potentials owing to this large degree of scatter in the data. However, it was noticed that once breakdown had initiated that further polarization of the specimens in the anodic direction under conditions of illumination did not lead to a reduction in the rate of attack; the anodic currents observed in the dark and in the light being of similar magnitude. This finding suggests that the inhibition of dissolution observed for the CA-715 and CDA-614 systems is more connected with a modification of the passive oxide film than any changes in the rate of the copper dis-

solution reactions in the chloride-containing solution.

4. Discussion

The data presented show that the resistance to dissolution of the copper-containing alloys, CA-715 and CDA-614 in dilute chloride solutions can be enhanced on illuminating the immersed electrodes with UV light, in the wavelength region 300–400 nm. Although illumination has only a small effect on the potential at which breakdown is first observed, with the noble displacement in the breakdown potential being of the order of 30 ± 25 mV and 25 ± 20 mV for CA-715 and CDA-614, respectively, illumination decreases considerably the rate at which further sites become activated.

It can be seen from the data presented in Fig. 4 that illumination of the surface during the early stages of the polarization measurements, in the potential interval -200 to $+190$ mV(SCE), is sufficient to induce changes in the passive film that render it more resistant to attack. This, coupled with the fact that illumination seemed to have little effect on the rate of the copper dissolution reactions in chloride solution, suggests that the observed enhanced resistance to dissolution is associated with some modification of the passive films that exist under these conditions. Secondly, it is seen that the presence of nickel in the alloy, or in the passive film, is not a prerequisite for this passivation-induced photo effect, as similar effects are observed with the CA-715 and CDA-614 alloys.

It is well known that the composition and development of passive layers on Cu–Ni and other copper alloys is dependent on parameters such as the applied potential, pH and time of formation [11, 27]. It is also known that the pitting susceptibility of the alloys depends on the nature of the passive film, and that variations in the manner in which the film is grown affect the breakdown process [27]. Thus, it is possible that the observed photo-induced passivation effect may be connected with alterations in the composition of the passive film where these alterations, or modifications, are facilitated, or accelerated, by illuminating the electrode.

However, an alternative attractive and viable mechanism to account for these observations involves viewing the complex oxide layer as a semiconductor and using the point defect model [28, 29] to describe the breakdown of passivity. On illuminating these semiconductor oxide films with sufficiently energetic photons, electrons are promoted from the valence to the conduction band generating electron–hole pairs or electron-ionized center pairs. These electron–hole pairs become separated with the holes and electrons moving in opposite directions. This separation of charge gives rise to a counter field, so that the electric field strength within the passive layer is quenched. This situation persists only while the electrode is illuminated, but this process is predicted [30] to modify the vacancy structure, which is much slower to relax [29], and would account for the persistence of the photo-induced passivation effect, Fig. 4. Since this modification of the vacancy structure depends on the quenching of the electric field strength [30], it is justified to postulate that the fundamental origin is quenching of the electric field strength.

The effects of a decrease in the electric field strength on the susceptibility of the alloy films to undergo localized attack can be seen from Eqs. (1) and (2), where the breakdown potential, V_b, and the induction period, t_{ind}, are expressed in terms of the electric field strength and transport of the vacancies in accordance with the point defect model [28, 29],

$$V_b = \frac{4.606RT}{\chi F\alpha}\log\left(\frac{J_m}{J^0 u^{-\chi/2}}\right) - \frac{2.303RT}{\alpha F}\log(a_{x^-}) \quad (1)$$

and

$$t_{ind} = \xi'\left[\exp\left(\frac{\chi\alpha F\Delta V}{2RT}\right) - 1\right]^{-1} + \tau, \quad (2)$$

where a_{x^-} is the activity of the aggressive anion in the solution, t_{ind} is the induction period, $\Delta V = V_{app} - V_b$, V_{app} is the applied potential, χ is the oxide stoichiometry ($MO_{\chi/2}$), α is the dependence of the potential difference across the film/solution interface on the applied potential, J_m is the rate of annihilation of cation vacancies at the metal/film interface, ξ' is related to the critical concentration of cation vacancies (ξ) at the metal/film interface through Eq. (3), and τ is defined as the time of dissolution of the cap above the cation vacancy condensate to the extent required for mechanical instability and rupture. J^0 and ξ' are defined by the following equations:

$$\xi' = \xi J^0 u^{-\chi/2}(a_{x^-})^{\chi/2}\exp\left(\frac{\chi\alpha FV_c}{2RT}\right) \quad (3)$$

and

$$J^0 = \chi\frac{\hat{\varepsilon}F}{RT}D\left(\frac{N_V}{\Omega}\right)^{1+\chi/2}\exp\left(\frac{-\Delta G_s^0}{RT}\right). \quad (4)$$

It can be seen from Eqs. (1) and (4) that a decrease in the electric field strength, $\hat{\varepsilon}$, leads to an increase in V_b, the breakdown potential. Also, ξ' is inversely proportional to $\hat{\varepsilon}$ [through J^0, Eq. (4)], so that a decrease in $\hat{\varepsilon}$ leads to an increase in t_{ind} [Eq. (2)]. This would account for the slight ennoblement in the breakdown potentials and the longer induction periods observed on illumination of the CA-715 and CDA-614 alloys.

It is clearly evident from the data presented in Fig. 4 that prior illumination of the electrodes reduces, to a greater extent, the rate at which the electrodes become further activated once the initial activation event has occurred. The increasing currents observed on polarizing the electrodes in the anodic direction both under illumination and non-illumination conditions are in part connected with the propagation of activated sites and the activation of new corroding sites. The propagation of active sites contributes increasingly to the observed current as the potential is made more positive and it would appear that the random current fluctuations, evident at current densities exceeding 210 μA cm^{-2}, are a result of propagation and the precipitation of the resultant corrosion products. However, the fact that the density of the corroding sites increased initially with increasing applied potential, as described in Section 3, seems to suggest that the activation of new corroding sites is the predominant event, at least during the early stages of potentiodynamic polarization. Thus, the difference in the current for the illuminated and non-illuminated electrodes, at lower current densities, is connected with the activation of new sites, where slightly longer induction periods are observed for the activation of successive additional sites on the illuminated electrodes.

This observation may be explained by assuming that the potential breakdown sites on the surface are normally distributed in terms of the cation vacancy diffusivity at these sites. Using this approach, it can be shown that the distributions in the induction time are given by [29]

$$\frac{\mathrm{d}N}{\mathrm{d}t_{\mathrm{ind}}} = \left(\frac{\xi u^{\chi/2}}{\sqrt{2\pi}\sigma_D \hat{a}}\right) \mathrm{e}^{-(D-\bar{D})^2/2\sigma_D^2} \frac{\mathrm{e}^{-\gamma V}}{(a_{x^-})^{\chi/2}(t_{\mathrm{ind}}-\tau)^2}, \qquad (5)$$

where

$$\bar{a} = \chi\left(\frac{\hat{\varepsilon}F}{RT}\right)\left(\frac{N_V}{\Omega}\right)^{1+\chi/2} \mathrm{e}^{-(\Delta G^0_s/RT)} \qquad (6)$$

and

$$\gamma = \chi F\alpha/2RT. \qquad (7)$$

Here, $\bar{D}$ is the mean diffusivity and σ_D is the standard deviation in the diffusivity. It can be seen from Eq. (6) that a decrease in $\hat{\varepsilon}$ will result in a decrease in the value of the parameter $\hat{a}$, which when entered into Eq. (5) will alter the differential cumulative distribution in induction time as defined by Eq. (8), where $\Delta N|_{t_J}^{t_{J+1}}$ is the number of sites that breakdown at voltage V between times t_J and t_{J+1},

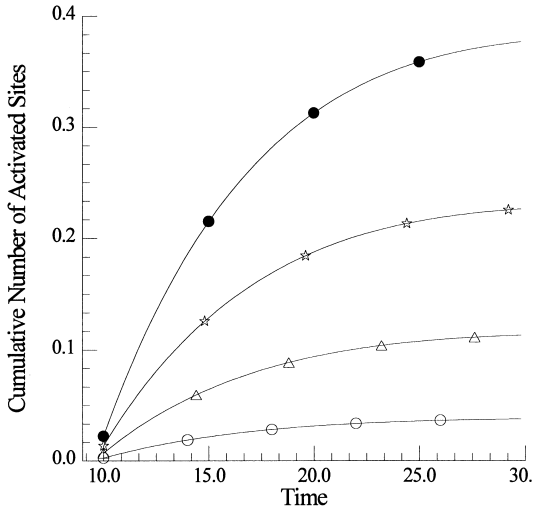

Fig. 6. Simulated data showing the number of activated sites as a function of the elapsed observation time for scaled $\hat{a}$ values of (●) 1.0, (☆) 0.6, (△) 0.3 and (○) 0.1.

$$\Delta N|_{t_J}^{t_{J+1}} = \int_{t_J}^{t_{J+1}} \left(\frac{\mathrm{d}N}{\mathrm{d}t_{\mathrm{ind}}}\right)\mathrm{d}t. \qquad (8)$$

The influence of the electric field strength, $\hat{\varepsilon}$, on this cumulative distribution in induction times, and therefore the onset of activation events, is best seen by the simulation shown in Fig. 6 which was constructed using Eq. (5). Here, the parameters t_{ind}, D and V were allowed to vary, where t_{ind} was treated as the observation time and is used to define the x axis in Fig. 6. The other parameters in Eq. (5) were treated as constants and were given a value of unity. The parameter D was allowed to vary between a value of 1 and 3, $\bar{D}$ was set to a value of 2 and σ_D to a value of 1. The induction time, t_{ind}, was allowed to vary from a value of 10 to 30 and V was varied between 1 and 2.08. The cumulative number of events activated at a given observation time (which is equivalent to the activation of the events after the elapse of a given induction time) was then obtained by summing the number of events, $\Delta N|_{t_J}^{t_{J+1}}$, between two observation times t_J and t_{J+1}. This represents the cumulative number of sites activated, which is shown on the y-axis in Fig. 6. The effects of variations in the electric field strength can then be seen by varying the parameter $\hat{a}$. It is clearly evident from these simulated data that a decrease in $\hat{a}$, which is equivalent to a decrease in $\hat{\varepsilon}$, leads to the activation of much fewer sites at any given time and that the rate of activation of new sites is also reduced.

Although some of the activated sites may become passivated and will not contribute to the current flow, the tendency of these copper-based alloys to undergo repassivation in chloride-containing solutions is small. Thus, it seems reasonable to assume that the current flow is proportional to the cumulative number of activated sites. If the potential axes in Figs. 1–4 are viewed in terms of observation time, then it can be seen that the simulated data exhibit features that are similar to the experimentally obtained data. Thus, the activation of fewer sites at any given time and the slower rate at which new sites become activated under illumination conditions is consistent with a quenching of the electric field strength.

5. Conclusions

The influence of UV light (300–450 nm) on the passive and dissolution behavior of CA-715 and CDA-614 in a dilute buffered chloride-containing solution was studied. On illuminating the immersed electrodes a slight ennoblement in the breakdown potential, and an increase in the induction time and reduced anodic current densities at potentials higher that the initial breakdown potential, were observed. These effects could be observed on continuous illumination of the immersed electrodes or if the electrodes were previously polarized under illumination conditions while in the passive state and then polarized into the active region under non-illumination conditions. These findings were explained in terms of a photo-induced quenching of the electric field strength and a consequent modification of the vacancy structure within the passive films, which in accordance with the point defect model accounts for the observed photo-inhibition of passivity breakdown.

Acknowledgements

The authors gratefully acknowledge the support of this work by the Electric Power Research Institute under Contract Number RP8041-07.

References

[1] H. H. Strehblow, B. Titze, Electrochim. Acta 25 (1980) 839.
[2] M. Novak, A. Szucs, J. Electroanal. Chem. 210 (1986) 229.
[3] U. Bertocci, J. Electrochem. Soc. 125 (1986) 415.
[4] M. Yamashita, K. Omura, D. Hirayama, Surf. Sci. 96 (1980) 443.
[5] C. Kato, B. G. Ateya, J. E. Castle, H. W. Pickering, J. Electrochem. Soc. 127 (1980) 1890.
[6] S. M. Wilhelm, Y. Tanizawa, C. Y. Liu, N. Hackerman, Corros. Sci. 22 (1986) 791.
[7] T. D. Burleigh, Corrosion 45 (1989) 464.
[8] C. Kato, B. G. Ateya, J. E. Castle, H. W. Pickering, J. Electrochem. Soc. 127 (1980) 1897.
[9] M. E. Walton, P. A. Brook, Corros. Sci. 17 (1977) 317.
[10] D. D. Macdonald, B. C. Syrett, S. S. Wing, Corrosion 34 (1978) 289.
[11] P. Druska, H.-H. Strehblow, Corrosion Sci. 38 (1996) 1369.
[12] J. A. Duffy, Bonding, Energy Levels and Bands in Inorganic Solids, Wiley, New York, 1990, p. 136.
[13] U. Bertocci, J. Electrochem. Soc. 125 (1978) 1598.
[14] W. Paatsch, Ber. Bunsenges. Phys. Chem. 81 (1977) 645.
[15] S. Sathiyanarayanan, S. P. Manoharan, G. Rajagopal, K. Balakrishnan, Br. Corros. J. 27 (1992) 72.
[16] J. Kruger, J. Electrochem. Soc. 106 (1959) 864.
[17] E. Escalante, J. Kruger, J. Electrochem. Soc. 118 (1971) 1062.
[18] W. Siripala, K. P. Kumara, Semicond. Sci. Technol. 4 (1989) 465.
[19] A. D. Modestov, G. D. Zhou, H. H. Ge, B. H. Loo, J. Electroanal. Chem. 380 (1995) 63.
[20] E. M. M. Sutter, B. Millet, C. Fiaud, D. Lincot, J. Electroanal. Chem. 386 (1995) 101.
[21] H. A. Arbit, K. Nobe, Corrosion (1968) 17.
[22] S. J. Lenhart, M. Urquidi-Macdonald, D. D. Macdonald, Electrochim. Acta 32 (1987) 1739.
[23] P. Schmuki, H. Böhni, Electrochim. Acta 40 (1995) 775.
[24] D. D. Macdonald, E. Sikora, M. W. Balmas, R. C. Alkire, Corros. Sci. 38 (1) (1996) 97.
[25] C. B. Breslin, D. D. Macdonald, E. Sikora, J. Sikora, Electrochim. Acta 42 (1997) 127.
[26] C. B. Breslin, D. D. Macdonald, E. Sikora, J. Sikora, Electrochim. Acta 42 (1997) 137.
[27] I. Milosev, M. Metikos-Hukovic, Corrosion 48 (1992) 185.
[28] L. F. Lin, C. Y. Chao, D. D. Macdonald, J. Electrochem. Soc. 128 (1981) 1194.
[29] D. D. Macdonald, in preparation (1997).
[30] D. D. Macdonald, J. Electrochem. Soc. 139 (1992) 3434.